

Observation of strangeness enhancement with charmed mesons in high-multiplicity $p\text{Pb}$ collisions at $\sqrt{s_{\text{NN}}} = 8.16$ TeV

R. Aaij *et al.**
(LHCb Collaboration)

 (Received 16 November 2023; accepted 8 July 2024; published 22 August 2024)

The production of prompt D_s^+ and D^+ mesons is measured by the LHCb experiment in proton-lead ($p\text{Pb}$) collisions in both the forward ($1.5 < y^* < 4.0$) and backward ($-5.0 < y^* < -2.5$) rapidity regions at a nucleon-nucleon center-of-mass energy of $\sqrt{s_{\text{NN}}} = 8.16$ TeV. The nuclear modification factors of both D_s^+ and D^+ mesons are determined as a function of transverse momentum, p_{T} , and rapidity. In addition, the D_s^+ to D^+ cross section ratio is measured as a function of the primary charged particle multiplicity in the event. An enhanced D_s^+ to D^+ production in high-multiplicity events is observed for the whole measured p_{T} range, in particular at low p_{T} and backward rapidity, where the significance exceeds six standard deviations. This constitutes the first observation of strangeness enhancement in charm quark hadronization in high-multiplicity $p\text{Pb}$ collisions. The results are also qualitatively consistent with the presence of quark coalescence as an additional charm quark hadronization mechanism in high-multiplicity proton-lead collisions.

DOI: [10.1103/PhysRevD.110.L031105](https://doi.org/10.1103/PhysRevD.110.L031105)

At hadron colliders, charm quarks are mainly produced by hard parton-parton interactions in the initial stages of the collisions, which are well described by perturbative quantum chromodynamics calculations. These calculations are based on the factorization theorem, according to which the charmed hadron cross sections are dependent on the parton distribution functions (PDFs) of the incoming nucleons, the hard parton-parton scattering cross section, and the fragmentation functions [1,2].

In proton-lead collisions, various effects could modify the charmed hadron cross sections compared to pp collisions. In the initial state, the charmed hadron production can be affected by the modification of the parton distribution functions of bound nucleons (nPDFs) [3,4] compared to those of free nucleons. Furthermore, the increased gluon density at small momentum fraction x leads to nonperturbative features, even if the coupling constant is weak. The color-glass condensate (CGC) effective theory [5,6] provides an appropriate theoretical framework in this regime. A recent measurement from the LHCb experiment has shown a discrepancy with the theoretical calculations based on nPDFs [7]. In the final state, the fragmentation functions are typically parametrized based on measurements

performed in e^+e^- or ep collisions, assuming that the hadronization of charm quarks to charmed hadrons is a universal process independent of the colliding system [8]. A recent measurement from the ALICE experiment has shown that charm quark hadronization differs between e^+e^- and pp collisions [9,10]. This result suggests the existence of other hadronization mechanisms beyond fragmentation. An alternative mechanism is quark coalescence [11–14], where charm quarks recombine with other quarks to form charmed hadrons. This mechanism requires that multiple quarks overlap in velocity-position space. As a result, the fraction of charmed hadrons produced by coalescence is expected to be larger when the number of quarks produced in the collision is large, for example in relativistic heavy-ion collisions where quark-gluon plasma (QGP) is formed [15,16]. This mechanism is also expected to be more prominent at relatively low transverse momentum, p_{T} , as most quarks or particles are produced in that kinematic region.

Relativistic heavy-ion collisions are often accompanied by strangeness enhancement, which was originally considered as a signature of QGP [17]. The enhanced strangeness production [18,19] and the coalescence mechanism result in an increased yield of strange charmed mesons relative to nonstrange charmed mesons compared to pp collisions [20,21]. Additionally, the ALICE collaboration observed the production enhancement of strange light hadrons in both high-multiplicity pp [22] and $p\text{Pb}$ [23,24] collisions. Although the origin of the strangeness enhancement in “small” systems (proton-proton or proton-nucleus collisions) is still under debate [25,26], it may

*Full author list given at the end of the article.

Published by the American Physical Society under the terms of the [Creative Commons Attribution 4.0 International license](https://creativecommons.org/licenses/by/4.0/). Further distribution of this work must maintain attribution to the author(s) and the published article's title, journal citation, and DOI. Funded by SCOAP³.

indicate a common underlying physics mechanism which gradually compensates the strangeness suppression in fragmentation. If the coalescence mechanism contributes to the charm quark hadronization in small systems, the production rates of D_s^+ mesons ($c\bar{s}$) relative to D^+ mesons ($c\bar{d}$) could also increase with the event multiplicity.

This Letter reports LHCb measurements of the prompt $D_{(s)}^+$ (D_s^+ and D^+) differential production cross sections, of their nuclear modification factors and forward-backward cross section ratio in p Pb collisions at $\sqrt{s_{\text{NN}}} = 8.16$ TeV. Additionally, the cross section ratio, $\sigma_{D_s^+}/\sigma_{D^+}$, as a function of the primary charged particle multiplicity of the events is reported.

The LHCb detector is a single-arm forward spectrometer covering the pseudorapidity range $2 < \eta < 5$, described in detail in Refs. [27,28]. The present measurement covers the forward rapidity range of $1.5 < y^* < 4.0$ when the proton beam points towards the LHCb arm, and the backward rapidity range of $-5.0 < y^* < -2.5$ when the lead beam does. Here, y^* is the rapidity in the nucleon-nucleon center-of-mass frame. The center-of-mass frame does not coincide with the laboratory frame due to the asymmetry of the colliding beam energies, with a constant boost of $y_{\text{lab}} - y^* = 0.5 \log(A/Z) = 0.465$ in the direction of the proton beam, where $A = 208$ is the lead nucleus mass number and $Z = 82$ is the lead nucleus atomic number. The corresponding integrated luminosity for the forward (backward) rapidity data sample is $12.18 \pm 0.32 \text{ nb}^{-1}$ ($18.57 \pm 0.46 \text{ nb}^{-1}$).

Simulation is used to model the effects of detector acceptance and selection requirements. The $D_{(s)}^+$ mesons are generated using PYTHIA 8 [29] and embedded into minimum-bias (MB) p Pb events using the EPOS generator [30], calibrated with LHC data [31]. The decays of unstable particles are described by EVTGEN [32], in which final-state radiation is generated using PHOTOS [33]. The interaction of the generated particles with the detector, and its response, are implemented using the GEANT8 toolkit [34] as described in Ref. [35]. The simulated $D_{(s)}^+$ event multiplicity distribution is weighted to match the background-subtracted distribution that is extracted from data using the *sPlot* method [36].

The double-differential cross section in a given (p_T, y^*) interval is defined as

$$\frac{d^2\sigma_{p\text{Pb}}}{dp_T dy^*} = \frac{N}{\mathcal{L} \times \epsilon^{\text{acc}} \times \epsilon^{\text{trig}} \times \epsilon^{\text{PID}} \times \epsilon^{\text{rec\&sel}} \times \mathcal{B} \times \Delta p_T \times \Delta y^*}, \quad (1)$$

where N is the observed number of prompt $D_{(s)}^+$ and $D_{(s)}^-$ mesons, \mathcal{L} the integrated luminosity, \mathcal{B} the branching fraction of the corresponding $D_{(s)}^+$ meson decay, ϵ^{acc} , ϵ^{trig} , ϵ^{PID} , $\epsilon^{\text{rec\&sel}}$ are the LHCb acceptance, trigger, particle identification (PID), reconstruction and selection efficiencies, respectively, and Δp_T and Δy^* are the p_T and y^*

interval widths. The $D_{(s)}^+$ mesons are reconstructed through the $D^+ \rightarrow K^- \pi^+ \pi^+$ and $D_s^+ \rightarrow K^- K^+ \pi^+$ decay channels, where the mass of the $K^+ K^-$ pair is required to be within $20 \text{ MeV}/c^2$ of the known mass of the $\phi(1020)$ meson. The corresponding branching fractions are $\mathcal{B} = (2.24 \pm 0.13)\%$ for the $D_s^+ \rightarrow K^- K^+ \pi^+$ decay [37], and $\mathcal{B} = (9.38 \pm 0.16)\%$ for the $D^+ \rightarrow K^- \pi^+ \pi^+$ decay [38].

The selection criteria applied to $D_{(s)}^+$ candidates are similar to those used in the recent D^0 production measurements in p Pb collisions at $\sqrt{s_{\text{NN}}} = 8.16$ TeV [7].

The sample of $D_{(s)}^+$ candidates includes $D_{(s)}^+$ mesons originating from the collision point and from the decay of b hadrons. These categories are referred to as ‘‘prompt’’ and ‘‘from- b ,’’ respectively. The inclusive signal yield is determined using an extended unbinned maximum-likelihood fit to the invariant-mass distributions of the $K^- K^+ \pi^+$ or $K^- \pi^+ \pi^+$ combinations. The invariant mass of the signal is described by the sum of a Crystal Ball function [39] and a Gaussian function, where both functions share a common mean, while the background shape is described by a linear function. The prompt signal yield is determined by fitting the distribution of $\log_{10}(\chi_{\text{IP}}^2)$ of the candidates, where χ_{IP}^2 is defined as the difference in the vertex-fit χ^2 of a given primary vertex (PV) reconstructed with and without the candidate under consideration. Combinatorial background in the $\log_{10}(\chi_{\text{IP}}^2)$ distribution is subtracted using the *sPlot* method with the charm meson invariant mass as discriminating variable. The shapes of the $\log_{10}(\chi_{\text{IP}}^2)$ distributions corresponding to the prompt and from- b components are described by Bukin functions [40]. The parameters of the function describing the from- b component are fixed from simulation, and the parameters describing the prompt component are allowed to float. Typical invariant mass and $\log_{10}(\chi_{\text{IP}}^2)$ distributions are shown in the Supplemental Material [41].

The LHCb acceptance, trigger, reconstruction, and selection efficiencies are evaluated with p Pb simulated samples. The track reconstruction efficiency is calibrated with MB $J/\psi \rightarrow \mu^+ \mu^-$ and $K_S^0 \rightarrow \pi^+ \pi^-$ samples, using the tag-and-probe approach of Ref. [42]. The PID efficiencies are estimated using a tag-and-probe method [43,44].

The various sources of systematic uncertainties considered in this measurement are listed in Table I. The uncertainty from the invariant mass fit is determined by describing signal and background shapes with alternative models [45]. For the estimation of the uncertainty associated to the $\log_{10}(\chi_{\text{IP}}^2)$ fit, the data are fitted again with different models and after varying any fixed parameters to evaluate the change in signal yield. The uncertainties on the tracking and PID calibration are dominated by the limited size of calibration samples. The uncertainty associated to the simulation multiplicity correction is estimated by weighting simulated events using different multiplicity variables. The larger uncertainty from multiplicity

TABLE I. Systematic uncertainties on the measured double-differential cross section. Each range indicates the minimum and the maximum value across all kinematic intervals. The uncertainties due to the mass and $\log_{10}(\chi^2_{\text{IP}})$ fits are uncorrelated across the intervals. The other sources of uncertainty are 100% correlated between the different intervals.

Uncertainty source	Forward [%]	Backward [%]
Mass fit	0.1–6.1	0.1–9.6
$\log_{10}(\chi^2_{\text{IP}})$ fit	0.1–22.2	0.1–17.3
Tracking calibration	0.9–3.6	1.4–9.6
PID calibration	1.2–14.0	1.4–8.9
Multiplicity correction	0.5–3.5	4.9–11.3
Trigger efficiency	0.0–1.6	0.0–1.5
Luminosity	2.6	2.5
Branching fraction D_s^+	5.8	5.8
Branching fraction D^+	1.7	1.7

corrections in the backward region primarily stems from a worse agreement between simulation and data in that region. For the trigger efficiency, the difference between the efficiencies derived from simulation and from collision

data [46] are considered as a systematic uncertainty. The uncertainties associated to the luminosity, the branching fractions and the simulated samples size are also included.

The double-differential cross sections for prompt D_s^+ (D^+) mesons are measured in the p_T range $1 < p_T < 13$ GeV/ c ($1 < p_T < 14$ GeV/ c) and the rapidity ranges $1.5 < y^* < 4.0$ and $-5.0 < y^* < -2.5$ for the forward and backward rapidity regions, respectively. The results and numerical values are given in the Supplemental Material [41]. The total prompt $D_{(s)}^+$ production cross sections, obtained by integrating the double-differential results in the measured kinematic ranges, are $42.83 \pm 0.29 \pm 3.45$ mb ($92.36 \pm 0.18 \pm 4.96$ mb) for the forward rapidity region, and $42.96 \pm 0.36 \pm 4.91$ mb ($84.09 \pm 0.17 \pm 8.39$ mb) for the backward rapidity region, where the first uncertainty is statistical and the second systematic.

The nuclear modification factor $R_{p\text{Pb}}$ is defined as the ratio of differential cross sections

$$R_{p\text{Pb}}(p_T, y^*) \equiv \frac{1}{A} \frac{d^2\sigma_{p\text{Pb}}(p_T, y^*)/(dp_T dy^*)}{d^2\sigma_{pp}(p_T, y^*)/(dp_T dy^*)}, \quad (2)$$

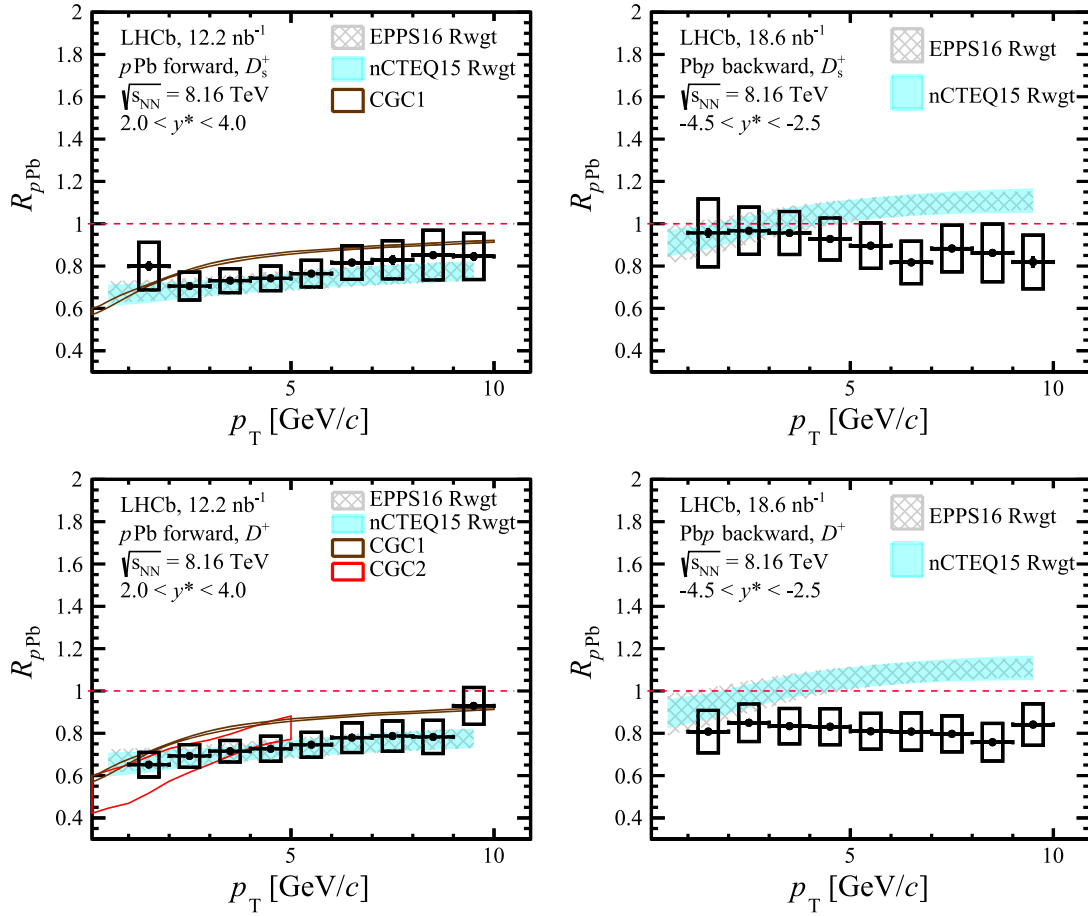


FIG. 1. Nuclear modification factor $R_{p\text{Pb}}$ as a function of p_T for prompt (upper) D_s^+ and (lower) D^+ mesons. Forward rapidity results are shown on the left and backward rapidity on the right. The vertical error bars show the statistical uncertainties and the boxes show the systematic uncertainties. The theoretical calculations are also shown [49–53].

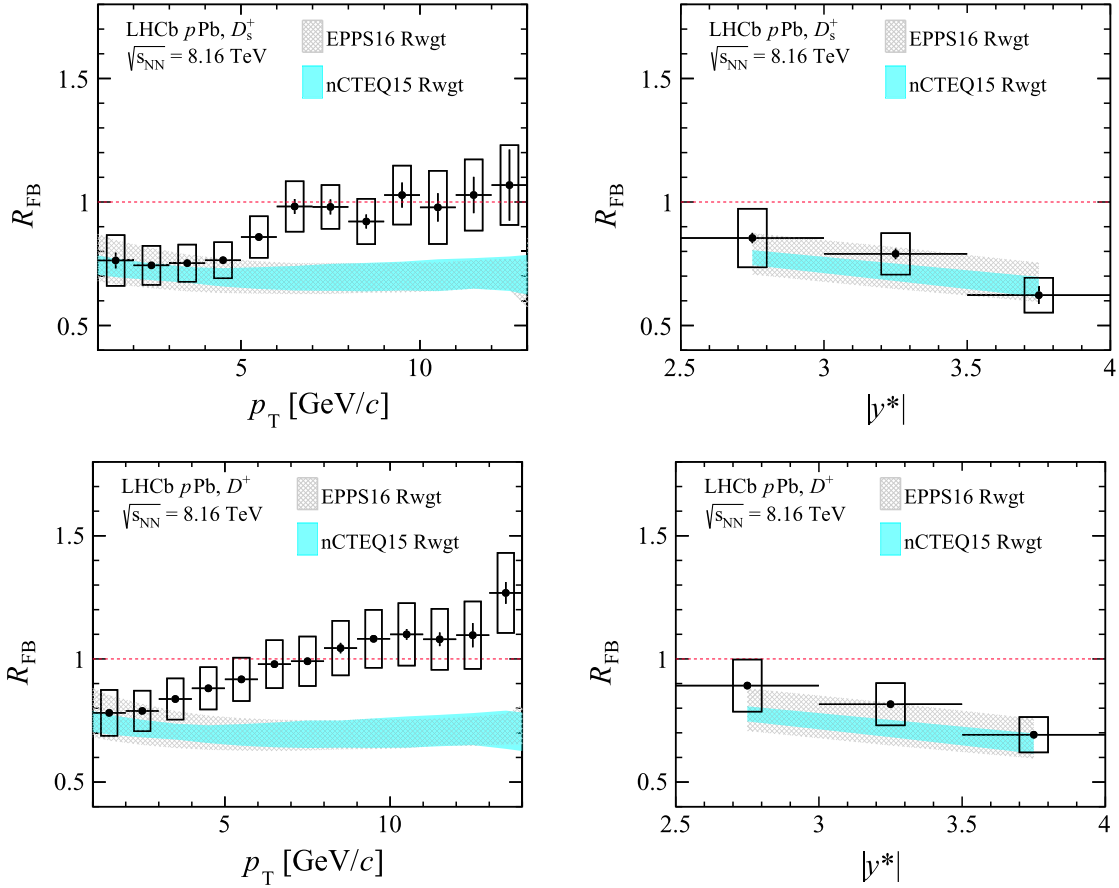


FIG. 2. Forward-backward cross-section ratio R_{FB} for prompt (upper) D_s^+ and (lower) D^+ mesons as a function of (left) p_T and (right) y^* . The vertical error bars show the statistical uncertainties and the boxes show the systematic uncertainties. The colored bands represent the theoretical calculations, incorporating nPDFs EPPS16 (gray) [52] and nCTEQ15 (cyan) [53].

where $A = 208$ is the lead nucleus mass number and σ_{pp} is the prompt $D_{(s)}^+$ meson cross section in pp collisions at $\sqrt{s} = 8.16$ TeV. The latter are obtained by an interpolation between LHCb measurements at $\sqrt{s} = 5.02$ TeV and $\sqrt{s} = 13$ TeV [47,48]. The interpolation is performed within the common kinematic range $1 < p_T < 10$ GeV/c and $2.0 < y < 4.5$, using a power-law function. The difference obtained when using a linear function is assigned as a systematic uncertainty.

The nuclear modification factors for $D_{(s)}^+$ mesons as a function of p_T are displayed in Fig. 1, where the results are integrated over the rapidity range $2.0 < y^* < 4.0$ for the forward rapidity region and $-4.5 < y^* < -2.5$ for the backward region. A significant suppression of $D_{(s)}^+$ production in pPb collisions, with respect to those in pp collisions scaled by the lead mass number, is observed at forward rapidity. Figures showing R_{pPb} in different y^* intervals of width $\Delta y^* = 0.5$, as well as the numerical values, are given in the Supplemental Material [41].

The R_{pPb} results are compared with nPDF theoretical calculations. These calculations use the HELAC-Onia approach [54,55], which is based on a data-driven modeling

of the scattering at partonic level folded with free proton PDFs [56]. They are first tuned by fitting the cross sections measured in pp collisions at the LHC. Then, the modified PDFs of nucleons in the Pb nucleus are introduced to calculate the cross sections in pPb collisions and to estimate the effect of nPDFs. Reweighted EPPS16 [52] or nCTEQ15 [53] nPDF sets, which incorporate LHC heavy-flavor data [57–60] in a Bayesian-reweighting analysis [61], are used in these calculations. This procedure leads to considerably reduced uncertainties with respect to calculations using the default nPDFs. The theoretical uncertainties shown in Fig. 1 are dominated by the nPDF parametrizations and correspond to a 68% confidence interval. At forward rapidity, the calculations are in satisfactory agreement with data. At backward rapidity, the data are lower than the calculations, indicating a weaker antishadowing effect or possible final-state effects that depend weakly on charm hadronization.

The nuclear modification factors in the forward rapidity region (small momentum fraction x) are also compared with two calculations based on the CGC effective field theory, CGC1 [49,50] and CGC2 [51]. The most significant theoretical uncertainty in CGC2 is the initial saturation

scale of the target nucleus. The CGC1 predictions have much smaller uncertainties than the CGC2 predictions, as they include only variations of the charm quark mass and of the factorization scale, which largely cancel out in the $R_{p\text{Pb}}$ ratio. The CGC1 calculations are consistent with the upper bound of the CGC2 predictions and slightly overshoot the data. The CGC2 predictions show a stronger suppression than HELAC-Onia, especially for $p_T < 3$ GeV/ c .

The forward-backward cross section ratio R_{FB} is defined as

$$R_{\text{FB}}(p_T, |y^*|) = \frac{d^2\sigma_{p\text{Pb}}(p_T, +|y^*|)/(dp_T dy^*)}{d^2\sigma_{p\text{Pb}}(p_T, -|y^*|)/(dp_T dy^*)}, \quad (3)$$

and calculated in the common $|y^*|$ interval of the forward-backward acceptances, namely $2.5 < |y^*| < 4$. The measurements of R_{FB} are shown as a function of p_T and $|y^*|$ in Fig. 2, along with the nPDF calculations [52,53]. Good agreement with nPDF calculations is found at low p_T ; however, the data show a clear rising trend with increasing p_T , reaching unity at the highest p_T values. This is in contrast to the nPDF calculations, which predict $R_{\text{FB}} \sim 0.7$ almost independently of p_T . This discrepancy originates from the observed suppression of high- p_T $D_{(s)}^+$ mesons at backward rapidity.

The cross-section ratio $\sigma_{D_s^+}/\sigma_{D^+}$, which is written as

$$\frac{\sigma_{D_s^+}}{\sigma_{D^+}} = \frac{N_{D_s^+}}{N_{D^+}} \times \frac{\mathcal{B}_{D^+}}{\mathcal{B}_{D_s^+}} \times \frac{\epsilon_{D^+}^{\text{acc}}}{\epsilon_{D_s^+}^{\text{acc}}} \times \frac{\epsilon_{D^+}^{\text{trig}}}{\epsilon_{D_s^+}^{\text{trig}}} \times \frac{\epsilon_{D^+}^{\text{PID}}}{\epsilon_{D_s^+}^{\text{PID}}} \times \frac{\epsilon_{D^+}^{\text{rec\&sel}}}{\epsilon_{D_s^+}^{\text{rec\&sel}}}, \quad (4)$$

is more precisely measured thanks to a cancellation of systematic uncertainties. The dependence of $\sigma_{D_s^+}/\sigma_{D^+}$ versus the primary charged particle multiplicity is measured in the $D_{(s)}^+$ kinematic intervals $2 < p_T < 12$ GeV/ c and $1.8 < y^* < 3.3$ ($-4.3 < y^* < -2.8$) for forward (backward) rapidity. The primary charged particle multiplicity, denoted as N_{ch} , represents the number of charged particles originating from the collisions, including decay products. In this Letter, it is estimated within the forward-pseudorapidity region ($2 < \eta < 4.8$) by measuring the number of tracks used to reconstruct the primary vertex, denoted as $N_{\text{Tracks}}^{\text{PV}}$. The correlation between the measured $N_{\text{Tracks}}^{\text{PV}}$ and N_{ch} is obtained from simulation.

Figure 3 shows the dependence of $\sigma_{D_s^+}/\sigma_{D^+}$ on primary charged particle multiplicity in four different p_T intervals (integrated over rapidity). Plots of $\sigma_{D_s^+}/\sigma_{D^+}$ in different y^* intervals and the derived numerical values are given in the Supplemental Material [41]. These measurements show that the $\sigma_{D_s^+}/\sigma_{D^+}$ ratio increases significantly as a function of the primary charged particle multiplicity, especially in the low- p_T and backward rapidity regions. They deviate

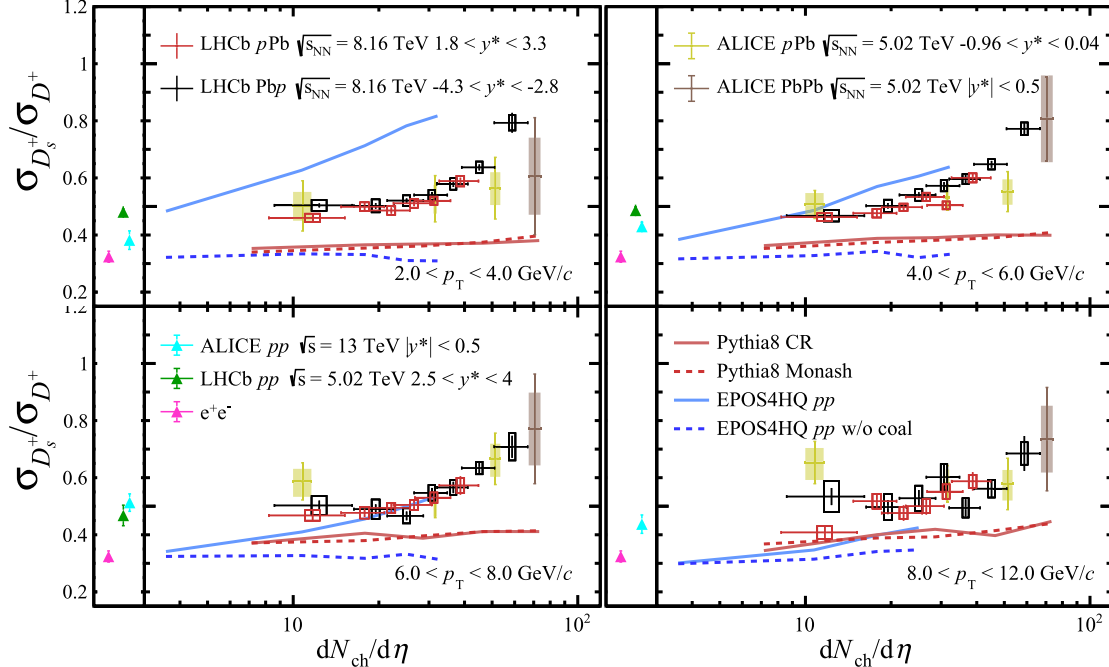


FIG. 3. Cross section ratio $\sigma_{D_s^+}/\sigma_{D^+}$ versus the primary charged particles per unit of pseudorapidity in e^+e^- [62], pp [10,63], $p\text{Pb}$ [64], PbPb [65] collisions in different $D_{(s)}^+$ p_T ranges. The vertical error bars show the statistical uncertainties and the boxes show the systematic uncertainties. The colored bands contain both statistical and systematic uncertainties. The calculations from PYTHIA 8 [66,67], EPOS4HQ [68,69], and EPOS4HQ without coalescence mechanism are also shown. These calculations are applicable to pp collisions at $\sqrt{s} = 8.16$ TeV within the rapidity range of $1.8 < y^* < 3.3$.

from a flat distribution, expected if only the fragmentation mechanism is considered, by 6.1 ($2 < p_T < 4$ GeV/c), 6.8 ($4 < p_T < 6$ GeV/c), 2.7 ($6 < p_T < 8$ GeV/c), and 3.2 ($8 < p_T < 12$ GeV/c) standard deviations in the forward rapidity region, and by 7.9 ($2 < p_T < 4$ GeV/c), 10.5 ($4 < p_T < 6$ GeV/c), 4.4 ($6 < p_T < 8$ GeV/c), and 1.1 ($8 < p_T < 12$ GeV/c) standard deviations at backward rapidity. As a comparison, the measured $\sigma_{D_s^+}/\sigma_{D^+}$ ratios in e^+e^- [62], pp [10,63], pPb [64], and $PbPb$ [65] collisions are also shown in the Fig. 3. There are significant differences in the $\sigma_{D_s^+}/\sigma_{D^+}$ ratios between pp and $PbPb$ collisions. The LHCb measurements reveal a trend where the ratio tends to resemble that of pp collisions in low-multiplicity pPb collisions, while it converges towards the behavior observed in $PbPb$ collisions in high-multiplicity pPb collisions. In pPb collisions, the LHCb data are compatible with the ratio measured by ALICE within uncertainties. The $\sigma_{D_s^+}/\sigma_{D^+}$ pattern is similar in both the forward and backward rapidity regions. This suggests that the $\sigma_{D_s^+}/\sigma_{D^+}$ ratio is independent of rapidity, and the mechanism contributing to this ratio increase is strongly correlated with the charged particle density. Additionally, theoretical calculations are compared using PYTHIA 8 with Monash [66] and CR [67] tunes, along with EPOS4HQ [68,69]. EPOS4HQ extends the EPOS4 framework to include heavy quarks and incorporates a coalescence mechanism in hadronization. These calculations are applicable to pp collisions. Theoretical calculations from PYTHIA 8 underestimate experimental measurements and do not fully capture the trends dependent on multiplicity. While EPOS4HQ also exhibits some discrepancies with experimental data, it can depict the multiplicity-dependent trends across all p_T intervals by introducing a coalescence mechanism.

In summary, the prompt $D_{(s)}^+$ production cross sections are measured by the LHCb experiment in pPb collisions at $\sqrt{s_{NN}} = 8.16$ TeV, both in the forward and backward rapidity regions. The nuclear modification factors are measured and found to be consistent with the previous results with D^0 mesons [7]. The results show a strong suppression of the $D_{(s)}^+$ cross sections at forward rapidity, consistent with the nPDF and CGC effective theory calculations. At backward rapidity, the R_{pPb} values of $D_{(s)}^+$ mesons are lower than nPDF calculations at high

p_T , indicating a weaker antishadowing effect than predicted by the models or additional hadronization-independent final-state effects. Moreover, the forward-backward cross-section ratio also shows a deviation from the nPDF calculations at high p_T . Combined with the nuclear modification factors, this deviation may arise from the observed suppression of high- p_T $D_{(s)}^+$ mesons at backward rapidity. The production of D_s^+ mesons is significantly enhanced relative to D^+ mesons in high particle multiplicity proton-lead collision events, in particular for low p_T and backward rapidity. This is the first observation of strangeness enhancement in charm quark hadronization in high-multiplicity small collision systems. The multiplicity-dependent trend is well understood within EPOS4HQ.

We express our gratitude to our colleagues in the CERN accelerator departments for the excellent performance of the LHC. We thank the technical and administrative staff at the LHCb institutes. We acknowledge support from CERN and from the national agencies: CAPES, CNPq, FAPERJ, and FINEP (Brazil); MOST and NSFC (China); CNRS/IN2P3 (France); BMBF, DFG, and MPG (Germany); INFN (Italy); NWO (Netherlands); MNiSW and NCN (Poland); MCID/IFA (Romania); MICINN (Spain); SNSF and SER (Switzerland); NASU (Ukraine); STFC (United Kingdom); DOE NP and NSF (USA). We acknowledge the computing resources that are provided by CERN, IN2P3 (France), KIT and DESY (Germany), INFN (Italy), SURF (Netherlands), PIC (Spain), GridPP (United Kingdom), CSCS (Switzerland), IFIN-HH (Romania), CBPF (Brazil), and Polish WLCG (Poland). We are indebted to the communities behind the multiple open-source software packages on which we depend. Individual groups or members have received support from ARC and ARDC (Australia); Key Research Program of Frontier Sciences of CAS, CAS PIFI, CAS CCEPP, Fundamental Research Funds for the Central Universities, and Sci. & Tech. Program of Guangzhou (China); Minciencias (Colombia); EPLANET, Marie Skłodowska-Curie Actions, ERC and NextGenerationEU (European Union); A*MIDEX, ANR, IPhU and Labex P2IO, and Région Auvergne-Rhône-Alpes (France); AvH Foundation (Germany); ICSC (Italy); GVA, XuntaGal, GENCAT, Inditex, InTalent and Prog. Atracción Talento, CM (Spain); SRC (Sweden); the Leverhulme Trust, the Royal Society and UKRI (United Kingdom).

[1] B.R. Webber, A QCD model for jet fragmentation including soft gluon interference, *Nucl. Phys.* **B238**, 492 (1984).

[2] B. Andersson, G. Gustafson, G. Ingelman, and T. Sjostrand, Parton fragmentation and string dynamics, *Phys. Rep.* **97**, 31 (1983).

- [3] M. Hirai, S. Kumano, and T.-H. Nagai, Determination of nuclear parton distribution functions and their uncertainties in next-to-leading order, *Phys. Rev. C* **76**, 065207 (2007).
- [4] K. J. Eskola, P. Paakkinen, H. Paukkunen, and C. A. Salgado, EPPS21: A global QCD analysis of nuclear PDFs, *Eur. Phys. J. C* **82**, 413 (2022).
- [5] F. Gelis, Color glass condensate and glasma, *Int. J. Mod. Phys. A* **28**, 1330001 (2013).
- [6] H. Fujii and K. Watanabe, Heavy quark pair production in high energy pA collisions: Open heavy flavors, *Nucl. Phys. A* **920**, 78 (2013).
- [7] I. Bezshyiko *et al.* (LHCb Collaboration), Measurement of the prompt D^0 nuclear modification factor in p-Pb collisions at $s_{NN} = 8.16$ TeV, *Phys. Rev. Lett.* **131**, 102301 (2023).
- [8] E. Braaten, K.-m. Cheung, S. Fleming, and T. C. Yuan, Perturbative QCD fragmentation functions as a model for heavy quark fragmentation, *Phys. Rev. D* **51**, 4819 (1995).
- [9] S. Acharya *et al.* (ALICE Collaboration), Charm-quark fragmentation fractions and production cross section at midrapidity in pp collisions at the LHC, *Phys. Rev. D* **105**, L011103 (2022).
- [10] S. Acharya *et al.* (ALICE Collaboration), Charm production and fragmentation fractions at midrapidity in pp collisions at $\sqrt{s} = 13$ TeV, *J. High Energy Phys.* **12** (2023) 086.
- [11] Y. Oh, C. M. Ko, S. H. Lee, and S. Yasui, Heavy baryon/meson ratios in relativistic heavy ion collisions, *Phys. Rev. C* **79**, 044905 (2009).
- [12] M. He and R. Rapp, Hadronization and charm-hadron ratios in heavy-ion collisions, *Phys. Rev. Lett.* **124**, 042301 (2020).
- [13] V. Minissale, S. Plumari, and V. Greco, Charm hadrons in pp collisions at LHC energy within a coalescence plus fragmentation approach, *Phys. Lett. B* **821**, 136622 (2021).
- [14] A. M. Sirunyan *et al.* (CMS Collaboration), Elliptic flow of charm and strange hadrons in high-multiplicity pPb collisions at $\sqrt{s_{NN}} = 8.16$ TeV, *Phys. Rev. Lett.* **121**, 082301 (2018).
- [15] J. Adams *et al.* (STAR Collaboration), Experimental and theoretical challenges in the search for the quark gluon plasma: The STAR Collaboration's critical assessment of the evidence from RHIC collisions, *Nucl. Phys. A* **757**, 102 (2005).
- [16] K. Adcox *et al.* (PHENIX Collaboration), Formation of dense partonic matter in relativistic nucleus-nucleus collisions at RHIC: Experimental evaluation by the PHENIX Collaboration, *Nucl. Phys. A* **757**, 184 (2005).
- [17] J. Rafelski and B. Müller, Strangeness production in the quark-gluon plasma, *Phys. Rev. Lett.* **48**, 1066 (1982).
- [18] G. Agakishiev *et al.* (STAR Collaboration), Strangeness enhancement in Cu + Cu and Au + Au collisions at $\sqrt{s_{NN}} = 200$ GeV, *Phys. Rev. Lett.* **108**, 072301 (2012).
- [19] B. B. Abelev *et al.* (ALICE Collaboration), Multi-strange baryon production at mid-rapidity in Pb-Pb collisions at $\sqrt{s_{NN}} = 2.76$ TeV, *Phys. Lett. B* **728**, 216 (2014); **734**, 409(E) (2014).
- [20] J. Adam *et al.* (STAR Collaboration), Observation of D_s^\pm/D^0 enhancement in Au + Au collisions at $\sqrt{s_{NN}} = 200$ GeV, *Phys. Rev. Lett.* **127**, 092301 (2021).
- [21] S. Acharya *et al.* (ALICE Collaboration), Measurement of prompt D_s^+ -meson production and azimuthal anisotropy in Pb-Pb collisions at $\sqrt{s_{NN}} = 5.02$ TeV, *Phys. Lett. B* **827**, 136986 (2022).
- [22] J. Adam *et al.* (ALICE Collaboration), Enhanced production of multi-strange hadrons in high-multiplicity proton-proton collisions, *Nat. Phys.* **13**, 535 (2017).
- [23] B. B. Abelev *et al.* (ALICE Collaboration), Multiplicity dependence of pion, kaon, proton and lambda production in p-Pb collisions at $\sqrt{s_{NN}} = 5.02$ TeV, *Phys. Lett. B* **728**, 25 (2014).
- [24] J. Adam *et al.* (ALICE Collaboration), Multi-strange baryon production in p-Pb collisions at $\sqrt{s_{NN}} = 5.02$ TeV, *Phys. Lett. B* **758**, 389 (2016).
- [25] Y. Kanakubo, Y. Tachibana, and T. Hirano, Unified description of hadron yield ratios from dynamical core-corona initialization, *Phys. Rev. C* **101**, 024912 (2020).
- [26] C. Bierlich, S. Chakraborty, G. Gustafson, and L. Lönnblad, Strangeness enhancement across collision systems without a plasma, *Phys. Lett. B* **835**, 137571 (2022).
- [27] A. A. Alves Jr. *et al.* (LHCb Collaboration), The LHCb detector at the LHC, *J. Instrum.* **3**, S08005 (2008).
- [28] R. Aaij *et al.* (LHCb Collaboration), LHCb detector performance, *Int. J. Mod. Phys. A* **30**, 1530022 (2015).
- [29] T. Sjöstrand, S. Mrenna, and P. Skands, A brief introduction to PYTHIA 8.1, *Comput. Phys. Commun.* **178**, 852 (2008); T. Sjöstrand, S. Mrenna, and P. Skands, PYTHIA 6.4 physics and manual, *J. High Energy Phys.* **05** (2006) 026.
- [30] T. Pierog, Iu. Karpenko, J. M. Katzy, E. Yatsenko, and K. Werner, EPOS LHC: Test of collective hadronization with data measured at the CERN Large Hadron Collider, *Phys. Rev. C* **92**, 034906 (2015).
- [31] I. Belyaev *et al.* (LHCb Collaboration), Handling of the generation of primary events in Gauss, the LHCb simulation framework, *J. Phys. Conf. Ser.* **331**, 032047 (2011).
- [32] D. J. Lange, The EvtGen particle decay simulation package, *Nucl. Instrum. Methods Phys. Res., Sect. A* **462**, 152 (2001).
- [33] P. Golonka and Z. Was, PHOTOS Monte Carlo: A precision tool for QED corrections in Z and W decays, *Eur. Phys. J. C* **45**, 97 (2006).
- [34] S. Agostinelli *et al.* (GEANT4 Collaboration), GEANT4—a simulation toolkit, *Nucl. Instrum. Methods Phys. Res., Sect. A* **506**, 250 (2003).
- [35] M. Clemencic *et al.* (LHCb Collaboration), The LHCb simulation application, Gauss: Design, evolution and experience, *J. Phys. Conf. Ser.* **331**, 032023 (2011).
- [36] M. Pivk and F. R. Le Diberder, sPlot: A statistical tool to unfold data distributions, *Nucl. Instrum. Methods Phys. Res., Sect. A* **555**, 356 (2005).
- [37] J. P. Alexander *et al.* (CLEO Collaboration), Absolute measurement of hadronic branching fractions of the D_s^+ meson, *Phys. Rev. Lett.* **100**, 161804 (2008).
- [38] R. L. Workman *et al.* (Particle Data Group), Review of particle physics, *Prog. Theor. Exp. Phys.* **2022**, 083C01 (2022).
- [39] T. Skwarnicki, A study of the radiative cascade transitions between the Upsilon-prime and Upsilon resonances, Ph.D. thesis, Institute of Nuclear Physics, Krakow, 1986 [Report No. DESY-F31-86-02], <http://inspirehep.net/record/230779/>.

- [40] A. D. Bukin, Fitting function for asymmetric peaks, [arXiv:0711.4449](https://arxiv.org/abs/0711.4449).
- [41] See the Supplemental Material at <http://link.aps.org/supplemental/10.1103/PhysRevD.110.L031105> for further details.
- [42] R. Aaij *et al.* (LHCb Collaboration), Measurement of the track reconstruction efficiency at LHCb, *J. Instrum.* **10**, P02007 (2015).
- [43] L. Anderlini *et al.*, The PIDCalib package, Report No. LHCb-PUB-2016-021, 2016, http://cdsweb.cern.ch/search?p=LHCb-PUB-2016-021&f=reportnumber&action_search=Search&c=LHCb+Notes.
- [44] R. Aaij *et al.*, Selection and processing of calibration samples to measure the particle identification performance of the LHCb experiment in Run 2, *Eur. Phys. J. Tech. Instrum.* **6**, 1 (2019).
- [45] I. Bezshyiko *et al.* (LHCb Collaboration), Measurement of prompt D^+ and D_s^+ production in pPb collisions at $\sqrt{s_{NN}} = 5.02$ TeV, *J. High Energy Phys.* **01** (2024) 070.
- [46] S. Tolk, J. Albrecht, F. Dettori, and A. Pellegrino, Data driven trigger efficiency determination at LHCb, Report No. LHCb-PUB-2014-039, 2014, http://cdsweb.cern.ch/search?p=LHCb-PUB-2014-039&f=reportnumber&action_search=Search&c=LHCb+Notes.
- [47] R. Aaij *et al.* (LHCb Collaboration), Measurements of prompt charm production cross-sections in $p p$ collisions at $\sqrt{s} = 5$ TeV, *J. High Energy Phys.* **06** (2017) 147.
- [48] R. Aaij *et al.* (LHCb Collaboration), Measurements of prompt charm production cross-sections in pp collisions at $\sqrt{s} = 13$ TeV, *J. High Energy Phys.* **03** (2016) 159; **09** (2016) 13; **05** (2017) 74.
- [49] B. Ducloué, T. Lappi, and H. Mäntysaari, Forward J/ψ production in proton-nucleus collisions at high energy, *Phys. Rev. D* **91**, 114005 (2015).
- [50] B. Ducloué, T. Lappi, and H. Mäntysaari, Forward J/ψ and D meson nuclear suppression at the LHC, *Nucl. Part. Phys. Proc.* **289–290**, 309 (2017).
- [51] Y.-Q. Ma, P. Tribedy, R. Venugopalan, and K. Watanabe, Event engineering studies for heavy flavor production and hadronization in high multiplicity hadron-hadron and hadron-nucleus collisions, *Phys. Rev. D* **98**, 074025 (2018).
- [52] K. J. Eskola, P. Paakkinen, H. Paukkunen, and C. A. Salgado, EPPS16: Nuclear parton distributions with LHC data, *Eur. Phys. J. C* **77**, 163 (2017).
- [53] K. Kovarik *et al.*, nCTEQ15—Global analysis of nuclear parton distributions with uncertainties in the CTEQ framework, *Phys. Rev. D* **93**, 085037 (2016).
- [54] H.-S. Shao, HELAC-Onia: An automatic matrix element generator for heavy quarkonium physics, *Comput. Phys. Commun.* **184**, 2562 (2013).
- [55] H.-S. Shao, HELAC-Onia 2.0: An upgraded matrix-element and event generator for heavy quarkonium physics, *Comput. Phys. Commun.* **198**, 238 (2016).
- [56] J.-P. Lansberg and H.-S. Shao, Towards an automated tool to evaluate the impact of the nuclear modification of the gluon density on quarkonium, D and B meson production in proton-nucleus collisions, *Eur. Phys. J. C* **77**, 1 (2017).
- [57] R. Aaij *et al.* (LHCb Collaboration), Study of prompt D^0 meson production in pPb collisions at $\sqrt{s_{NN}} = 5$ TeV, *J. High Energy Phys.* **10** (2017) 090.
- [58] B. B. Abelev *et al.* (ALICE Collaboration), Measurement of prompt D -meson production in p-Pb collisions at $\sqrt{s_{NN}} = 5.02$ TeV, *Phys. Rev. Lett.* **113**, 232301 (2014).
- [59] J. Adam *et al.* (ALICE Collaboration), Measurement of D -meson production versus multiplicity in p-Pb collisions at $\sqrt{s_{NN}} = 5.02$ TeV, *J. High Energy Phys.* **08** (2016) 078.
- [60] J. Adam *et al.* (ALICE Collaboration), D -meson production in p-Pb collisions at $\sqrt{s_{NN}} = 5.02$ TeV and in pp collisions at $\sqrt{s} = 7$ TeV, *Phys. Rev. C* **94**, 054908 (2016).
- [61] A. Kusina, J.-P. Lansberg, I. Schienbein, and H.-S. Shao, Gluon shadowing in heavy-flavor production at the LHC, *Phys. Rev. Lett.* **121**, 052004 (2018).
- [62] M. Lisovyi, A. Verbitskiy, and O. Zenaiev, Combined analysis of charm-quark fragmentation-fraction measurements, *Eur. Phys. J. C* **76**, 397 (2016).
- [63] R. Aaij *et al.* (LHCb Collaboration), Measurements of prompt charm production cross-sections in pp collisions at $\sqrt{s} = 5$ TeV, *J. High Energy Phys.* **06** (2017) 147.
- [64] S. Acharya *et al.* (ALICE Collaboration), Measurement of prompt D^0 , D^+ , D^{*+} , and D_s^+ production in p-Pb collisions at $\sqrt{s_{NN}} = 5.02$ TeV, *J. High Energy Phys.* **12** (2019) 092.
- [65] S. Acharya *et al.* (ALICE Collaboration), Measurement of D^0 , D^+ , D^{*+} and D_s^+ production in Pb-Pb collisions at $\sqrt{s_{NN}} = 5.02$ TeV, *J. High Energy Phys.* **10** (2018) 174.
- [66] P. Skands, S. Carrazza, and J. Rojo, Tuning PYTHIA 8.1: The Monash 2013 tune, *Eur. Phys. J. C* **74**, 3024 (2014).
- [67] J. R. Christiansen and P. Z. Skands, String formation beyond leading colour, *J. High Energy Phys.* **08** (2015) 003.
- [68] J. Zhao, J. Aichelin, P. B. Gossiaux, and K. Werner, Heavy flavor as a probe of hot QCD matter produced in proton-proton collisions, *Phys. Rev. D* **109**, 054011 (2024).
- [69] J. Zhao, J. Aichelin, P. B. Gossiaux, and K. Werner, Heavy flavour hadron production in relativistic heavy ion collisions at RHIC and LHC in EPOS4HQ, [arXiv:2401.17096](https://arxiv.org/abs/2401.17096).

R. Aaij³⁵, A. S. W. Abdelmotteleb⁵⁴, C. Abellan Beteta⁴⁸, F. Abudinén⁵⁴, T. Ackernley⁵⁸, B. Adeva⁴⁴, M. Adinolfi⁵², P. Adlarson⁷⁸, H. Afsharnia¹¹, C. Agapopoulou⁴⁶, C. A. Aidala⁷⁹, Z. Ajaltouni¹¹, S. Akar⁶³, K. Akiba³⁵, P. Albicocco²⁵, J. Albrecht¹⁷, F. Alessio⁴⁶, M. Alexander⁵⁷, A. Alfonso Albero⁴³, Z. Aliouche⁶⁰, P. Alvarez Cartelle⁵³, R. Amalric¹⁵, S. Amato³, J. L. Amey⁵², Y. Amhis^{13,46}, L. An⁶, L. Anderlini²⁴, M. Andersson⁴⁸, A. Andreianov⁴¹, P. Andreola⁴⁸, M. Andreotti²³, D. Andreou⁶⁶, D. Ao⁷, F. Archilli^{34,b}, S. Argüedas Cuendis⁹, A. Artamonov⁴¹, M. Artuso⁶⁶, E. Aslanides¹², M. Atzeni⁶², B. Audurier¹⁴, D. Bacher⁶¹, I. Bachiller Perea¹⁰, S. Bachmann¹⁹, M. Bachmayer⁴⁷, J. J. Back⁵⁴, A. Bailly-reyre¹⁵, P. Baladron Rodriguez⁴⁴

V. Balagura¹⁴ W. Baldini^{23,46} J. Baptista de Souza Leite² M. Barbetti^{24,c} I. R. Barbosa⁶⁷ R. J. Barlow⁶⁰
 S. Barsuk¹³ W. Barter⁵⁶ M. Bartolini⁵³ F. Baryshnikov⁴¹ J. M. Basels¹⁶ G. Bassi^{32,d} B. Batsukh⁵
 A. Battig¹⁷ A. Bay⁴⁷ A. Beck⁵⁴ M. Becker¹⁷ F. Bedeschi³² I. B. Bediaga² A. Beiter⁶⁶ S. Belin⁴⁴
 V. Bellee⁴⁸ K. Belous⁴¹ I. Belov²⁶ I. Belyaev⁴¹ G. Benane¹² G. Bencivenni²⁵ E. Ben-Haim¹⁵
 A. Berezhnoy⁴¹ R. Bernet⁴⁸ S. Bernet Andres⁴² D. Berninghoff¹⁹ H. C. Bernstein⁶⁶ C. Bertella⁶⁰ A. Bertolin³⁰
 C. Betancourt⁴⁸ F. Betti⁵⁶ J. Bex⁵³ Ia. Bezshyiko⁴⁸ J. Bhom³⁸ L. Bian⁷¹ M. S. Bieker¹⁷ N. V. Biesuz²³
 P. Billoir¹⁵ A. Biolchini³⁵ M. Birch⁵⁹ F. C. R. Bishop⁵³ A. Bitadze⁶⁰ A. Bizzeti⁶⁰ M. P. Blago⁵³ T. Blake⁵⁴
 F. Blanc⁴⁷ J. E. Blank¹⁷ S. Blusk⁶⁶ D. Bobulska⁵⁷ V. Bocharnikov⁴¹ J. A. Boelhauve¹⁷ O. Boente Garcia¹⁴
 T. Boettcher⁶³ A. Bohare⁵⁶ A. Boldyrev⁴¹ C. S. Bolognani⁷⁶ R. Bolzonella^{23,e} N. Bondar⁴¹ F. Borgato^{30,46}
 S. Borghi⁶⁰ M. Borsato^{28,f} J. T. Borsuk³⁸ S. A. Bouchiba⁴⁷ T. J. V. Bowcock⁵⁸ A. Boyer⁴⁶ C. Bozzi²³
 M. J. Bradley⁵⁹ S. Braun⁶⁴ A. Brea Rodriguez⁴⁴ N. Breer¹⁷ J. Brodzicka³⁸ A. Brossa Gonzalo⁴⁴ J. Brown⁵⁸
 D. Brundu²⁹ A. Buonauro⁴⁸ L. Buonincontri³⁰ A. T. Burke⁶⁰ C. Burr⁴⁶ A. Bursche⁶⁹ A. Butkevich⁴¹
 J. S. Butter⁵³ J. Buytaert⁴⁶ W. Byczynski⁴⁶ S. Cadeddu²⁹ H. Cai⁷¹ R. Calabrese^{23,e} L. Calefice¹⁷ S. Cali²⁵
 M. Calvi^{28,f} M. Calvo Gomez⁴² J. Cambon Bouzas⁴⁴ P. Campana²⁵ D. H. Campora Perez⁷⁶
 A. F. Campoverde Quezada⁷ S. Capelli^{28,f} L. Capriotti²³ A. Carbone^{22,g} L. Carcedo Salgado⁴⁴
 R. Cardinale^{26,h} A. Cardini²⁹ P. Carniti^{28,f} L. Carus¹⁹ A. Casais Vidal⁴⁴ R. Caspary¹⁹ G. Casse⁵⁸
 J. Castro Godinez⁹ M. Cattaneo⁴⁶ G. Cavallero²³ V. Cavallini^{23,e} S. Celani⁴⁷ J. Cerasoli¹² D. Cervenkov⁶¹
 S. Cesare^{27,i} A. J. Chadwick⁵⁸ I. Chahrour⁷⁹ M. G. Chapman⁵² M. Charles¹⁵ Ph. Charpentier⁴⁶
 C. A. Chavez Barajas⁵⁸ M. Chefdeville¹⁰ C. Chen¹² S. Chen⁵ A. Chernov³⁸ S. Chernyshenko⁵⁰
 V. Chobanova^{44,j} S. Cholak⁴⁷ M. Chruszcz³⁸ A. Chubykin⁴¹ V. Chulikov⁴¹ P. Ciambone²⁵ M. F. Cicala⁵⁴
 X. Cid Vidal⁴⁴ G. Ciezarek⁴⁶ P. Cifra⁴⁶ P. E. L. Clarke⁵⁶ M. Clemencic⁴⁶ H. V. Cliff⁵³ J. Closier⁴⁶
 J. L. Cobble Dick⁶⁰ C. Cocha Toapaxi¹⁹ V. Coco⁴⁶ J. Cogan¹² E. Cogneras¹¹ L. Cojocariu⁴⁰ P. Collins⁴⁶
 T. Colombo⁴⁶ A. Comerma-Montells⁴³ L. Congedo²¹ A. Contu²⁹ N. Cooke⁵⁷ I. Corredoira⁴⁴ A. Correia¹⁵
 G. Corti⁴⁶ J. J. Cottee Meldrum⁵² B. Couturier⁴⁶ D. C. Craik⁴⁸ M. Cruz Torres^{2,k} R. Currie⁵⁶ C. L. Da Silva⁶⁵
 S. Dadabaev⁴¹ L. Dai⁶⁸ X. Dai⁶ E. Dall'Occo¹⁷ J. Dalseno⁴⁴ C. D'Ambrosio⁴⁶ J. Daniel¹¹ A. Danilina⁴¹
 P. d'Argent²¹ A. Davidson⁵⁴ J. E. Davies⁶⁰ A. Davis⁶⁰ O. De Aguiar Francisco⁶⁰ C. De Angelis^{29,l}
 J. de Boer³⁵ K. De Bruyn⁷⁵ S. De Capua⁶⁰ M. De Cian¹⁹ U. De Freitas Carneiro Da Graca^{2,m} E. De Lucia²⁵
 J. M. De Miranda² L. De Paula³ M. De Serio^{21,n} D. De Simone⁴⁸ P. De Simone²⁵ F. De Vellis¹⁷
 J. A. de Vries⁷⁶ F. Debernardis^{21,n} D. Decamp¹⁰ V. Dedu¹² L. Del Buono¹⁵ B. Delaney⁶² H.-P. Dembinski¹⁷
 J. Deng⁸ V. Denysenko⁴⁸ O. Deschamps¹¹ F. Dettori^{29,l} B. Dey⁷⁴ P. Di Nezza²⁵ I. Diachkov⁴¹
 S. Didenko⁴¹ S. Ding⁶⁶ V. Dobishuk⁵⁰ A. D. Docheva⁵⁷ A. Dolmatov⁴¹ C. Dong⁴ A. M. Donohoe²⁰
 F. Dordei²⁹ A. C. dos Reis² L. Douglas⁵⁷ A. G. Downes¹⁰ W. Duan⁶⁹ P. Duda⁷⁷ M. W. Dudek³⁸
 L. Dufour⁴⁶ V. Duk³¹ P. Durante⁴⁶ M. M. Duras⁷⁷ J. M. Durham⁶⁵ D. Dutta⁶⁰ A. Dziurda³⁸ A. Dzyuba⁴¹
 S. Easo^{55,46} E. Eckstein⁷³ U. Egede¹ A. Egorychev⁴¹ V. Egorychev⁴¹ C. Eirea Orro⁴⁴ S. Eisenhardt⁵⁶
 E. Ejopu⁶⁰ S. Ek-In⁴⁷ L. Eklund⁷⁸ M. Elashri⁶³ J. Ellbracht¹⁷ S. Ely⁵⁹ A. Ene⁴⁰ E. Eppele⁶³ S. Escher¹⁶
 J. Eschle⁴⁸ S. Esen⁴⁸ T. Evans⁶⁰ F. Fabiano^{29,46,l} L. N. Falcao² Y. Fan⁷ B. Fang^{71,13} L. Fantini^{31,o}
 M. Faria⁴⁷ K. Farmer⁵⁶ D. Fazzini^{28,f} L. Felkowski⁷⁷ M. Feng^{5,7} M. Feo⁴⁶ M. Fernandez Gomez⁴⁴
 A. D. Fernez⁶⁴ F. Ferrari²² F. Ferreira Rodrigues³ S. Ferreres Sole³⁵ M. Ferrillo⁴⁸ M. Ferro-Luzzi⁴⁶
 S. Filippov⁴¹ R. A. Fini²¹ M. Fiorini^{23,e} M. Firlej³⁷ K. M. Fischer⁶¹ D. S. Fitzgerald⁷⁹ C. Fitzpatrick⁶⁰
 T. Fiutowski³⁷ F. Fleuret¹⁴ M. Fontana²² F. Fontanelli^{26,h} L. F. Foreman⁶⁰ R. Forty⁴⁶ D. Foulds-Holt⁵³
 M. Franco Sevilla⁶⁴ M. Frank⁴⁶ E. Franzoso^{23,e} G. Frau¹⁹ C. Frei⁴⁶ D. A. Friday⁶⁰ L. Frontini^{27,i} J. Fu⁷
 Q. Fuehring¹⁷ Y. Fujii¹ T. Fulghesu¹⁵ E. Gabriel³⁵ G. Galati^{21,n} M. D. Galati³⁵ A. Gallas Torreira⁴⁴
 D. Galli^{22,g} S. Gambetta^{56,46} M. Gandelman³ P. Gandini²⁷ H. Gao⁷ R. Gao⁶¹ Y. Gao⁸ Y. Gao⁶ Y. Gao⁸
 M. Garau^{29,l} L. M. Garcia Martin⁴⁷ P. Garcia Moreno⁴³ J. García Pardiñas⁴⁶ B. Garcia Plata⁴⁴
 F. A. Garcia Rosales¹⁴ L. Garrido⁴³ C. Gaspar⁴⁶ R. E. Geertsema³⁵ L. L. Gerken¹⁷ E. Gersabeck⁶⁰
 M. Gersabeck⁶⁰ T. Gershon⁵⁴ Z. Ghorbanimoghaddam⁵² L. Giambastiani³⁰ F. I. Giasemis^{15,p} V. Gibson⁵³
 H. K. Gienza³⁹ A. L. Gilman⁶¹ M. Giovannetti²⁵ A. Gioventù⁴³ P. Gironella Gironell⁴³ C. Giugliano^{23,e}
 M. A. Giza³⁸ K. Gizdov⁵⁶ E. L. Gkougkousis⁵⁹ F. C. Glaser^{13,19} V. V. Gligorov¹⁵ C. Göbel⁶⁷
 E. Golobardes⁴² D. Golubkov⁴¹ A. Golutvin^{59,41,46} A. Gomes^{2,a,q} S. Gomez Fernandez⁴³

F. Goncalves Abrantes⁶¹ M. Goncerz³⁸ G. Gong⁴ J. A. Gooding¹⁷ I. V. Gorelov⁴¹ C. Gotti²⁸
 J. P. Grabowski⁷³ L. A. Granado Cardoso⁴⁶ E. Graugés⁴³ E. Graverini⁴⁷ L. Grazette⁵⁴ G. Graziani⁹
 A. T. Grecu⁴⁰ L. M. Greeven³⁵ N. A. Grieser⁶³ L. Grillo⁵⁷ S. Gromov⁴¹ C. Gu¹⁴ M. Guarise²³
 M. Guittiere¹³ V. Guliaeva⁴¹ P. A. Günther¹⁹ A.-K. Guseinov⁴¹ E. Gushchin⁴¹ Y. Guz^{6,41,46} T. Gys⁴⁶
 T. Hadavizadeh¹ C. Hadjivasiliou⁶⁴ G. Haefeli⁴⁷ C. Haen⁴⁶ J. Haimberger⁴⁶ S. C. Haines⁵³ M. Hajheidari⁴⁶
 T. Halewood-leagas⁵⁸ M. M. Halvorsen⁴⁶ P. M. Hamilton⁶⁴ J. Hammerich⁵⁸ Q. Han⁸ X. Han¹⁹
 S. Hansmann-Menzemer¹⁹ L. Hao⁷ N. Harnew⁶¹ T. Harrison⁵⁸ M. Hartmann¹³ C. Hasse⁴⁶ J. He^{7,r}
 K. Heijhoff³⁵ F. Hemmer⁴⁶ C. Henderson⁶³ R. D. L. Henderson^{1,54} A. M. Hennequin⁴⁶ K. Hennessy⁵⁸
 L. Henry⁴⁷ J. Herd⁵⁹ J. Heuel¹⁶ A. Hicheur³ D. Hill⁴⁷ M. Hilton⁶⁰ S. E. Hollitt¹⁷ J. Horswill⁶⁰ R. Hou⁸
 Y. Hou¹⁰ N. Howarth⁵⁸ J. Hu¹⁹ J. Hu⁶⁹ W. Hu⁶ X. Hu⁴ W. Huang⁷ X. Huang⁷¹ W. Hulsbergen³⁵
 R. J. Hunter⁵⁴ M. Hushchyn⁴¹ D. Hutchcroft⁵⁸ P. Ibis¹⁷ M. Idzik³⁷ D. Ilin⁴¹ P. Iiten⁶³ A. Inglessi⁴¹
 A. Iniukhin⁴¹ A. Ishteev⁴¹ K. Ivshin⁴¹ R. Jacobsson⁴⁶ H. Jage¹⁶ S. J. Jaimes Elles^{45,72} S. Jakobsen⁴⁶
 E. Jans³⁵ B. K. Jashal⁴⁵ A. Jawahery⁶⁴ V. Jevtic¹⁷ E. Jiang⁶⁴ X. Jiang^{5,7} Y. Jiang⁷ Y. J. Jiang⁶ M. John⁶¹
 D. Johnson⁵¹ C. R. Jones⁵³ T. P. Jones⁵⁴ S. Joshi³⁹ B. Jost⁴⁶ N. Jurik⁴⁶ I. Juszcak³⁸ D. Kaminaris⁴⁷
 S. Kandybei⁴⁹ Y. Kang⁴ M. Karacson⁴⁶ D. Karpenkov⁴¹ M. Karpov⁴¹ A. M. Kauniskangas⁴⁷ J. W. Kautz⁶³
 F. Keizer⁴⁶ D. M. Keller⁶⁶ M. Kenzie⁵³ T. Ketel³⁵ B. Khanji⁶⁶ A. Kharisova⁴¹ S. Kholodenko³²
 G. Khreich¹³ T. Kirm¹⁶ V. S. Kirsebom⁴⁷ O. Kitouni⁶² S. Klaver³⁶ N. Kleijne^{32,d} K. Klimaszewski³⁹
 M. R. Kmiec³⁹ S. Koliiev⁵⁰ L. Kolk¹⁷ A. Konoplyannikov⁴¹ P. Kopciwicz^{37,46} P. Koppenburg³⁵
 M. Korolev⁴¹ I. Kostiuik³⁵ O. Kot⁵⁰ S. Kotriakhova⁴¹ A. Kozachuk⁴¹ P. Kravchenko⁴¹ L. Kravchuk⁴¹
 M. Kreps⁵⁴ S. Kretschmar¹⁶ P. Krokovny⁴¹ W. Krupa⁶⁶ W. Krzemien³⁹ J. Kubat¹⁹ S. Kubis⁷⁷
 W. Kucewicz³⁸ M. Kucharczyk³⁸ V. Kudryavtsev⁴¹ E. Kulikova⁴¹ A. Kupsc⁷⁸ B. K. Kutsenko¹²
 D. Lacarrere⁴⁶ G. Lafferty⁶⁰ A. Lai²⁹ A. Lampis^{29,1} D. Lancierini⁴⁸ C. Landesa Gomez⁴⁴ J. J. Lane¹
 R. Lane⁵² C. Langenbruch¹⁹ J. Langer¹⁷ O. Lantwin⁴¹ T. Latham⁵⁴ F. Lazzari^{32,s} C. Lazzeroni⁵¹
 R. Le Gac¹² S. H. Lee⁷⁹ R. Lefèvre¹¹ A. Leflat⁴¹ S. Legotin⁴¹ M. Lehuraux⁵⁴ O. Leroy¹² T. Lesiak³⁸
 B. Leverington¹⁹ A. Li⁴ H. Li⁶⁹ K. Li⁸ L. Li⁶⁰ P. Li⁴⁶ P.-R. Li⁷⁰ S. Li⁸ T. Li⁵ T. Li⁶⁹ Y. Li⁸ Y. Li⁵
 Z. Li⁶⁶ Z. Lian⁴ X. Liang⁶⁶ C. Lin⁷ T. Lin⁵⁵ R. Lindner⁴⁶ V. Lisovskyi⁴⁷ R. Litvinov^{29,1} G. Liu⁶⁹
 H. Liu⁷ K. Liu⁷⁰ Q. Liu⁷ S. Liu^{5,7} Y. Liu⁵⁶ Y. Liu⁷⁰ A. Lobo Salvia⁴³ A. Loi²⁹ J. Lomba Castro⁴⁴
 T. Long⁵³ I. Longstaff⁵⁷ J. H. Lopes³ A. Lopez Huertas⁴³ S. López Soliño⁴⁴ G. H. Lovell⁵³ Y. Lu^{5,t}
 C. Lucarelli^{24,c} D. Lucchesi^{30,u} S. Luchuk⁴¹ M. Lucio Martinez⁷⁶ V. Lukashenko^{35,50} Y. Luo⁴ A. Lupato³⁰
 E. Luppi^{23,e} K. Lynch²⁰ X.-R. Lyu⁷ G. M. Ma⁴ R. Ma⁷ S. Maccolini¹⁷ F. Machefer¹³ F. Maciuc⁴⁰
 I. Mackay⁶¹ L. R. Madhan Mohan⁵³ M. M. Madurai⁵¹ A. Maevskiy⁴¹ D. Magdalinski³⁵ D. Maisuzenko⁴¹
 M. W. Majewski³⁷ J. J. Malczewski³⁸ S. Malde⁶¹ B. Malecki^{38,46} L. Malentacca⁴⁶ A. Malinin⁴¹ T. Maltsev⁴¹
 G. Manca^{29,1} G. Mancinelli¹² C. Mancuso^{27,13,i} R. Manera Escalero⁴³ D. Manuzzi²² D. Marangotto^{27,i}
 J. F. Marchand¹⁰ U. Marconi²² S. Mariani⁴⁶ C. Marin Benito^{43,46} J. Marks¹⁹ A. M. Marshall⁵² P. J. Marshall⁵⁸
 G. Martelli^{31,o} G. Martellotti³³ L. Martinazzoli⁴⁶ M. Martinelli^{28,f} D. Martinez Santos⁴⁴ F. Martinez Vidal⁴⁵
 A. Massafferri² M. Materok¹⁶ R. Matev⁴⁶ A. Mathad⁴⁸ V. Matiunin⁴¹ C. Matteuzzi^{66,28} K. R. Mattioli¹⁴
 A. Mauri⁵⁹ E. Maurice¹⁴ J. Mauricio⁴³ M. Mazurek⁴⁶ M. McCann⁵⁹ L. McConnell²⁰ T. H. McGrath⁶⁰
 N. T. McHugh⁵⁷ A. McNab⁶⁰ R. McNulty²⁰ B. Meadows⁶³ G. Meier¹⁷ D. Melnychuk³⁹ M. Merk^{35,76}
 A. Merli^{27,i} L. Meyer Garcia³ D. Miao^{5,7} H. Miao⁷ M. Mikhasenko^{73,v} D. A. Milanese⁷² A. Minotti^{28,f}
 E. Minucci⁶⁶ T. Miralles¹¹ S. E. Mitchell⁵⁶ B. Mitreska¹⁷ D. S. Mitzel¹⁷ A. Modak⁵⁵ A. Mödden¹⁷
 R. A. Mohammed⁶¹ R. D. Moise¹⁶ S. Mokhnenko⁴¹ T. Mombächer⁴⁶ M. Monk^{54,1} I. A. Monroy⁷²
 S. Monteil¹¹ A. Morcillo Gomez⁴⁴ G. Morello²⁵ M. J. Morello^{32,d} M. P. Morgenthaler¹⁹ J. Moron³⁷
 A. B. Morris⁴⁶ A. G. Morris¹² R. Mountain⁶⁶ H. Mu⁴ Z. M. Mu⁶ E. Muhammad⁵⁴ F. Muheim⁵⁶
 M. Mulder⁷⁵ K. Müller⁴⁸ F. Muñoz-Rojas⁹ R. Murta⁵⁹ P. Naik⁵⁸ T. Nakada⁴⁷ R. Nandakumar⁵⁵
 T. Nanut⁴⁶ I. Nasteva³ M. Needham⁵⁶ N. Neri^{27,i} S. Neubert⁷³ N. Neufeld⁴⁶ P. Neustroev⁴¹ R. Newcombe⁵⁹
 J. Nicolini^{17,13} D. Nicotra⁷⁶ E. M. Niel⁴⁷ N. Nikitin⁴¹ P. Nogga⁷³ N. S. Nolte⁶² C. Normand^{10,29,1}
 J. Novoa Fernandez⁴⁴ G. Nowak⁶³ C. Nunez⁷⁹ H. N. Nur⁵⁷ A. Oblakowska-Mucha³⁷ V. Obraztsov⁴¹
 T. Oeser¹⁶ S. Okamura^{23,46,e} R. Oldeman^{29,1} F. Oliva⁵⁶ M. Olocco¹⁷ C. J. G. Onderwater⁷⁶ R. H. O'Neil⁵⁶
 J. M. Otorola Goicochea³ T. Ovsianikova⁴¹ P. Owen⁴⁸ A. Oyanguren⁴⁵ O. Ozcelik⁵⁶ K. O. Padeken⁷³

B. Pagare⁵⁴, P. R. Pais¹⁹, T. Pajero⁶¹, A. Palano²¹, M. Palutan²⁵, G. Panshin⁴¹, L. Paolucci⁵⁴, A. Papanestis⁵⁵,
 M. Pappagallo^{21,n}, L. L. Pappalardo^{23,e}, C. Pappenheimer⁶³, C. Parkes^{60,46}, B. Passalacqua^{23,e}, G. Passaleva²⁴,
 D. Passaro^{32,d}, A. Pastore²¹, M. Patel⁵⁹, J. Patoc⁶¹, C. Patrignani^{22,g}, C. J. Pawley⁷⁶, A. Pellegrino³⁵,
 M. Pepe Altarelli²⁵, S. Perazzini²², D. Pereima⁴¹, A. Pereiro Castro⁴⁴, P. Perret¹¹, A. Perro⁴⁶, K. Petridis⁵²,
 A. Petrolini^{26,h}, S. Petrucci⁵⁶, H. Pham⁶⁶, L. Pica^{32,d}, M. Piccini³¹, B. Pietrzyk¹⁰, G. Pietrzyk¹³, D. Pinci³³,
 F. Pisani⁴⁶, M. Pizzichemi^{28,f}, V. Placinta⁴⁰, M. Plo Casasus⁴⁴, F. Polci^{15,46}, M. Poli Lener²⁵, A. Poluektov¹²,
 N. Polukhina⁴¹, I. Polyakov⁴⁶, E. Polycarpo³, S. Ponce⁴⁶, D. Popov⁷, S. Poslavskii⁴¹, K. Prasanth³⁸,
 L. Promberger¹⁹, C. Prouve⁴⁴, V. Pugatch⁵⁰, V. Puill¹³, G. Punzi^{32,s}, H. R. Qi⁴, W. Qian⁷, N. Qin⁴, S. Qu⁴,
 R. Quagliani⁴⁷, B. Rachwal³⁷, J. H. Rademacker⁵², M. Rama³², M. Ramírez García⁷⁹, M. Ramos Pernas⁵⁴,
 M. S. Rangel³, F. Ratnikov⁴¹, G. Raven³⁶, M. Rebollo De Miguel⁴⁵, F. Redi⁴⁶, J. Reich⁵², F. Reiss⁶⁰, Z. Ren⁴,
 P. K. Resmi⁶¹, R. Ribatti^{32,d}, G. R. Ricart^{14,80}, D. Riccardi^{32,d}, S. Ricciardi⁵⁵, K. Richardson⁶²,
 M. Richardson-Slipper⁵⁶, K. Rinnert⁵⁸, P. Robbe¹³, G. Robertson⁵⁶, E. Rodrigues^{58,46}, E. Rodriguez Fernandez⁴⁴,
 J. A. Rodriguez Lopez⁷², E. Rodriguez Rodriguez⁴⁴, A. Rogovskiy⁵⁵, D. L. Rolf⁴⁶, A. Rollings⁶¹, P. Roloff⁴⁶,
 V. Romanovskiy⁴¹, M. Romero Lamas⁴⁴, A. Romero Vidal⁴⁴, G. Romolini²³, F. Ronchetti⁴⁷, M. Rotondo²⁵,
 S. R. Roy¹⁹, M. S. Rudolph⁶⁶, T. Ruf⁴⁶, R. A. Ruiz Fernandez⁴⁴, J. Ruiz Vidal^{78,w}, A. Ryzhikov⁴¹, J. Ryzka³⁷,
 J. J. Saborido Silva⁴⁴, R. Sadek¹⁴, N. Sagidova⁴¹, N. Sahoo⁵¹, B. Saitta^{29,1}, M. Salomoni⁴⁶, C. Sanchez Gras³⁵,
 I. Sanderswood⁴⁵, R. Santacesaria³³, C. Santamarina Rios⁴⁴, M. Santimaria²⁵, L. Santoro², E. Santovetti³⁴,
 D. Saranin⁴¹, G. Sarpis⁵⁶, M. Sarpis⁷³, A. Sarti³³, C. Satriano^{33,x}, A. Satta³⁴, M. Saur⁶, D. Savrina⁴¹,
 H. Sazak¹¹, L. G. Scantlebury Smead⁶¹, A. Scarabotto¹⁵, S. Schael¹⁶, S. Scherl⁵⁸, A. M. Schertz⁷⁴,
 M. Schiller⁵⁷, H. Schindler⁴⁶, M. Schmelling¹⁸, B. Schmidt⁴⁶, S. Schmitt¹⁶, H. Schmitz⁷³, O. Schneider⁴⁷,
 A. Schopper⁴⁶, N. Schulte¹⁷, S. Schulte⁴⁷, M. H. Schune¹³, R. Schwemmer⁴⁶, G. Schwering¹⁶, B. Sciascia²⁵,
 A. Sciuccati⁴⁶, S. Sellam⁴⁴, A. Semennikov⁴¹, M. Senghi Soares³⁶, A. Sergi^{26,h}, N. Serra^{48,46}, L. Sestini³⁰,
 A. Seuthe¹⁷, Y. Shang⁶, D. M. Shangase⁷⁹, M. Shapkin⁴¹, I. Shchemerov⁴¹, L. Shchutska⁴⁷, T. Shears⁵⁸,
 L. Shekhtman⁴¹, Z. Shen⁶, S. Sheng^{5,7}, V. Shevchenko⁴¹, B. Shi⁷, E. B. Shields^{28,f}, Y. Shimizu¹³,
 E. Shmanin⁴¹, R. Shorkin⁴¹, J. D. Shupperd⁶⁶, R. Silva Coutinho⁶⁶, G. Simi³⁰, S. Simone^{21,n}, M. Singla¹,
 N. Skidmore⁶⁰, R. Skuza¹⁹, T. Skwarnicki⁶⁶, M. W. Slater⁵¹, J. C. Smallwood⁶¹, J. G. Smeaton⁵³, E. Smith⁶²,
 K. Smith⁶⁵, M. Smith⁵⁹, A. Snoch³⁵, L. Soares Lavra⁵⁶, M. D. Sokoloff⁶³, F. J. P. Soler⁵⁷, A. Solomin^{41,52},
 A. Solovev⁴¹, I. Solovyev⁴¹, R. Song¹, Y. Song⁴⁷, Y. Song⁴, Y. S. Song⁶, F. L. Souza De Almeida³,
 B. Souza De Paula³, E. Spadaro Norella^{27,i}, E. Spedicato²², J. G. Speer¹⁷, E. Spiridenkov⁴¹, P. Spradlin⁵⁷,
 V. Sriskaran⁴⁶, F. Stagni⁴⁶, M. Stahl⁴⁶, S. Stahl⁴⁶, S. Stanislaus⁶¹, E. N. Stein⁴⁶, O. Steinkamp⁴⁸, O. Stenyakin⁴¹,
 H. Stevens¹⁷, D. Strelakina⁴¹, Y. Su⁷, F. Suljik⁶¹, J. Sun²⁹, L. Sun⁷¹, Y. Sun⁶⁴, P. N. Swallow⁵¹,
 K. Swientek³⁷, F. Swystun⁵⁴, A. Szabelski³⁹, T. Szumlak³⁷, M. Szymanski⁴⁶, Y. Tan⁴, S. Taneja⁶⁰, M. D. Tat⁶¹,
 A. Terentev⁴⁸, F. Terzuoli^{32,y}, F. Teubert⁴⁶, E. Thomas⁴⁶, D. J. D. Thompson⁵¹, H. Tilquin⁵⁹, V. Tisserand¹¹,
 S. T'Jampens¹⁰, M. Tobin⁵, L. Tomassetti^{23,e}, G. Tonani^{27,i}, X. Tong⁶, D. Torres Machado², L. Toscano¹⁷,
 D. Y. Tou⁴, C. Tripll⁴², G. Tuci¹⁹, N. Tuning³⁵, L. H. Uecker¹⁹, A. Ukleja³⁷, D. J. Unverzagt¹⁹, E. Ursov⁴¹,
 A. Usachov³⁶, A. Ustyuzhanin⁴¹, U. Uwer¹⁹, V. Vagnoni²², A. Valassi⁴⁶, G. Valenti²², N. Valls Canudas⁴²,
 M. Van Dijk⁴⁷, H. Van Hecke⁶⁵, E. van Herwijnen⁵⁹, C. B. Van Hulse^{44,z}, R. Van Laak⁴⁷, M. van Veghel³⁵,
 R. Vazquez Gomez⁴³, P. Vazquez Regueiro⁴⁴, C. Vázquez Sierra⁴⁴, S. Vecchi²³, J. J. Velthuis⁵², M. Veltri^{24,aa},
 A. Venkateswaran⁴⁷, M. Vesterinen⁵⁴, D. Vieira⁶³, M. Vieites Diaz⁴⁶, X. Vilasis-Cardona⁴², E. Vilella Figueras⁵⁸,
 A. Villa²², P. Vincent¹⁵, F. C. Volle¹³, D. vom Bruch¹², V. Vorobyev⁴¹, N. Voropaev⁴¹, K. Vos⁷⁶, C. Vrahas⁵⁶,
 J. Walsh³², E. J. Walton¹, G. Wan⁶, C. Wang¹⁹, G. Wang⁸, J. Wang⁶, J. Wang⁵, J. Wang⁴, J. Wang⁷¹,
 M. Wang²⁷, N. W. Wang⁷, R. Wang⁵², X. Wang⁶⁹, Y. Wang⁸, Z. Wang¹³, Z. Wang⁴, Z. Wang⁷, J. A. Ward^{54,1},
 N. K. Watson⁵¹, D. Websdale⁵⁹, Y. Wei⁶, B. D. C. Westhenry⁵², D. J. White⁶⁰, M. Whitehead⁵⁷,
 A. R. Wiederhold⁵⁴, D. Wiedner¹⁷, G. Wilkinson⁶¹, M. K. Wilkinson⁶³, M. Williams⁶², M. R. J. Williams⁵⁶,
 R. Williams⁵³, F. F. Wilson⁵⁵, W. Wislicki³⁹, M. Witek³⁸, L. Witola¹⁹, C. P. Wong⁶⁵, G. Wormser¹³,
 S. A. Wotton⁵³, H. Wu⁶⁶, J. Wu⁸, Y. Wu⁶, K. Wyllie⁴⁶, S. Xian⁶⁹, Z. Xiang⁵, Y. Xie⁸, A. Xu³², J. Xu⁷,
 L. Xu⁴, L. Xu⁴, M. Xu⁵⁴, Z. Xu¹¹, Z. Xu⁷, Z. Xu⁵, D. Yang⁴, S. Yang⁷, X. Yang⁶, Y. Yang^{26,h}, Z. Yang⁶,
 Z. Yang⁶⁴, V. Yeroshenko¹³, H. Yeung⁶⁰, H. Yin⁸, C. Y. Yu⁶, J. Yu⁶⁸, X. Yuan⁵, E. Zaffaroni⁴⁷,
 M. Zavertyaev¹⁸, M. Zdybal³⁸, M. Zeng⁴, C. Zhang⁶, D. Zhang⁸, J. Zhang⁷, L. Zhang⁴, S. Zhang⁶⁸

S. Zhang⁶,⁶ Y. Zhang⁶,⁶ Y. Zhang,⁶¹ Y. Z. Zhang⁴,⁴ Y. Zhao¹⁹,¹⁹ A. Zharkova⁴¹,⁴¹ A. Zhelezov¹⁹,¹⁹ X. Z. Zheng⁴,⁴
 Y. Zheng⁷,⁷ T. Zhou⁶,⁶ X. Zhou⁸,⁸ Y. Zhou⁷,⁷ V. Zhovkovska¹³,¹³ L. Z. Zhu⁷,⁷ X. Zhu⁴,⁴ X. Zhu⁸,⁸ Z. Zhu⁷,⁷
 V. Zhukov^{16,41},^{16,41} J. Zhuo⁴⁵,⁴⁵ Q. Zou^{5,7},^{5,7} S. Zucchelli^{22,g},^{22,g} D. Zuliani³⁰,³⁰ and G. Zunica⁶⁰

(LHCb Collaboration)

- ¹*School of Physics and Astronomy, Monash University, Melbourne, Australia*
²*Centro Brasileiro de Pesquisas Físicas (CBPF), Rio de Janeiro, Brazil*
³*Universidade Federal do Rio de Janeiro (UFRJ), Rio de Janeiro, Brazil*
⁴*Center for High Energy Physics, Tsinghua University, Beijing, China*
⁵*Institute Of High Energy Physics (IHEP), Beijing, China*
⁶*School of Physics State Key Laboratory of Nuclear Physics and Technology, Peking University, Beijing, China*
⁷*University of Chinese Academy of Sciences, Beijing, China*
⁸*Institute of Particle Physics, Central China Normal University, Wuhan, Hubei, China*
⁹*Consejo Nacional de Rectores (CONARE), San Jose, Costa Rica*
¹⁰*Université Savoie Mont Blanc, CNRS, IN2P3-LAPP, Annecy, France*
¹¹*Université Clermont Auvergne, CNRS/IN2P3, LPC, Clermont-Ferrand, France*
¹²*Aix Marseille Univ, CNRS/IN2P3, CPPM, Marseille, France*
¹³*Université Paris-Saclay, CNRS/IN2P3, IJCLab, Orsay, France*
¹⁴*Laboratoire Leprince-Ringuet, CNRS/IN2P3, Ecole Polytechnique, Institut Polytechnique de Paris, Palaiseau, France*
¹⁵*LPNHE, Sorbonne Université, Paris Diderot Sorbonne Paris Cité, CNRS/IN2P3, Paris, France*
¹⁶*I. Physikalisches Institut, RWTH Aachen University, Aachen, Germany*
¹⁷*Fakultät Physik, Technische Universität Dortmund, Dortmund, Germany*
¹⁸*Max-Planck-Institut für Kernphysik (MPIK), Heidelberg, Germany*
¹⁹*Physikalisches Institut, Ruprecht-Karls-Universität Heidelberg, Heidelberg, Germany*
²⁰*School of Physics, University College Dublin, Dublin, Ireland*
²¹*INFN Sezione di Bari, Bari, Italy*
²²*INFN Sezione di Bologna, Bologna, Italy*
²³*INFN Sezione di Ferrara, Ferrara, Italy*
²⁴*INFN Sezione di Firenze, Firenze, Italy*
²⁵*INFN Laboratori Nazionali di Frascati, Frascati, Italy*
²⁶*INFN Sezione di Genova, Genova, Italy*
²⁷*INFN Sezione di Milano, Milano, Italy*
²⁸*INFN Sezione di Milano-Bicocca, Milano, Italy*
²⁹*INFN Sezione di Cagliari, Monserrato, Italy*
³⁰*Università degli Studi di Padova, Università e INFN, Padova, Padova, Italy*
³¹*INFN Sezione di Perugia, Perugia, Italy*
³²*INFN Sezione di Pisa, Pisa, Italy*
³³*INFN Sezione di Roma La Sapienza, Roma, Italy*
³⁴*INFN Sezione di Roma Tor Vergata, Roma, Italy*
³⁵*Nikhef National Institute for Subatomic Physics, Amsterdam, Netherlands*
³⁶*Nikhef National Institute for Subatomic Physics and VU University Amsterdam, Amsterdam, Netherlands*
³⁷*AGH—University of Science and Technology, Faculty of Physics and Applied Computer Science, Kraków, Poland*
³⁸*Henryk Niewodniczanski Institute of Nuclear Physics Polish Academy of Sciences, Kraków, Poland*
³⁹*National Center for Nuclear Research (NCBJ), Warsaw, Poland*
⁴⁰*Horia Hulubei National Institute of Physics and Nuclear Engineering, Bucharest-Magurele, Romania*
⁴¹*Affiliated with an institute covered by a cooperation agreement with CERN*
⁴²*DS4DS, La Salle, Universitat Ramon Llull, Barcelona, Spain*
⁴³*ICCUB, Universitat de Barcelona, Barcelona, Spain*
⁴⁴*Instituto Galego de Física de Altas Enerxías (IGFAE), Universidade de Santiago de Compostela, Santiago de Compostela, Spain*
⁴⁵*Instituto de Física Corpuscular, Centro Mixto Universidad de Valencia—CSIC, Valencia, Spain*
⁴⁶*European Organization for Nuclear Research (CERN), Geneva, Switzerland*
⁴⁷*Institute of Physics, Ecole Polytechnique Fédérale de Lausanne (EPFL), Lausanne, Switzerland*
⁴⁸*Physik-Institut, Universität Zürich, Zürich, Switzerland*
⁴⁹*NSC Kharkiv Institute of Physics and Technology (NSC KIPT), Kharkiv, Ukraine*

- ⁵⁰*Institute for Nuclear Research of the National Academy of Sciences (KINR), Kyiv, Ukraine*
- ⁵¹*University of Birmingham, Birmingham, United Kingdom*
- ⁵²*H.H. Wills Physics Laboratory, University of Bristol, Bristol, United Kingdom*
- ⁵³*Cavendish Laboratory, University of Cambridge, Cambridge, United Kingdom*
- ⁵⁴*Department of Physics, University of Warwick, Coventry, United Kingdom*
- ⁵⁵*STFC Rutherford Appleton Laboratory, Didcot, United Kingdom*
- ⁵⁶*School of Physics and Astronomy, University of Edinburgh, Edinburgh, United Kingdom*
- ⁵⁷*School of Physics and Astronomy, University of Glasgow, Glasgow, United Kingdom*
- ⁵⁸*Oliver Lodge Laboratory, University of Liverpool, Liverpool, United Kingdom*
- ⁵⁹*Imperial College London, London, United Kingdom*
- ⁶⁰*Department of Physics and Astronomy, University of Manchester, Manchester, United Kingdom*
- ⁶¹*Department of Physics, University of Oxford, Oxford, United Kingdom*
- ⁶²*Massachusetts Institute of Technology, Cambridge, MA, United States*
- ⁶³*University of Cincinnati, Cincinnati, OH, United States*
- ⁶⁴*University of Maryland, College Park, MD, United States*
- ⁶⁵*Los Alamos National Laboratory (LANL), Los Alamos, NM, United States*
- ⁶⁶*Syracuse University, Syracuse, NY, United States*
- ⁶⁷*Pontifícia Universidade Católica do Rio de Janeiro (PUC-Rio), Rio de Janeiro, Brazil (associated with Universidade Federal do Rio de Janeiro (UFRJ), Rio de Janeiro, Brazil)*
- ⁶⁸*School of Physics and Electronics, Hunan University, Changsha City, China (associated with Institute of Particle Physics, Central China Normal University, Wuhan, Hubei, China)*
- ⁶⁹*Guangdong Provincial Key Laboratory of Nuclear Science, Guangdong-Hong Kong Joint Laboratory of Quantum Matter, Institute of Quantum Matter, South China Normal University, Guangzhou, China (associated with Center for High Energy Physics, Tsinghua University, Beijing, China)*
- ⁷⁰*Lanzhou University, Lanzhou, China (associated with Institute Of High Energy Physics (IHEP), Beijing, China)*
- ⁷¹*School of Physics and Technology, Wuhan University, Wuhan, China (associated with Center for High Energy Physics, Tsinghua University, Beijing, China)*
- ⁷²*Departamento de Física, Universidad Nacional de Colombia, Bogota, Colombia (associated with LPNHE, Sorbonne Université, Paris Diderot Sorbonne Paris Cité, CNRS/IN2P3, Paris, France)*
- ⁷³*Universität Bonn—Helmholtz-Institut für Strahlen und Kernphysik, Bonn, Germany (associated with Physikalisches Institut, Ruprecht-Karls-Universität Heidelberg, Heidelberg, Germany)*
- ⁷⁴*Eotvos Lorand University, Budapest, Hungary (associated with European Organization for Nuclear Research (CERN), Geneva, Switzerland)*
- ⁷⁵*Van Swinderen Institute, University of Groningen, Groningen, Netherlands (associated with Nikhef National Institute for Subatomic Physics, Amsterdam, Netherlands)*
- ⁷⁶*Universiteit Maastricht, Maastricht, Netherlands (associated with Nikhef National Institute for Subatomic Physics, Amsterdam, Netherlands)*
- ⁷⁷*Tadeusz Kosciuszko Cracow University of Technology, Cracow, Poland (associated with Henryk Niewodniczanski Institute of Nuclear Physics Polish Academy of Sciences, Kraków, Poland)*
- ⁷⁸*Department of Physics and Astronomy, Uppsala University, Uppsala, Sweden (associated with School of Physics and Astronomy, University of Glasgow, Glasgow, United Kingdom)*
- ⁷⁹*University of Michigan, Ann Arbor, MI, United States (associated with Syracuse University, Syracuse, NY, United States)*
- ⁸⁰*Departement de Physique Nucleaire (SPhN), Gif-Sur-Yvette, France*

^aDeceased.

^bAlso at Università di Roma Tor Vergata, Roma, Italy.

^cAlso at Università di Firenze, Firenze, Italy.

^dAlso at Scuola Normale Superiore, Pisa, Italy.

^eAlso at Università di Ferrara, Ferrara, Italy.

^fAlso at Università di Milano Bicocca, Milano, Italy.

^gAlso at Università di Bologna, Bologna, Italy.

^hAlso at Università di Genova, Genova, Italy.

ⁱAlso at Università degli Studi di Milano, Milano, Italy.

^jAlso at Universidad da Coruña, Coruña, Spain.

^kAlso at Universidad Nacional Autónoma de Honduras, Tegucigalpa, Honduras.

^lAlso at Università di Cagliari, Cagliari, Italy.

^mAlso at Centro Federal de Educação Tecnológica Celso Suckow da Fonseca, Rio De Janeiro, Brazil.

ⁿAlso at Università di Bari, Bari, Italy.

^oAlso at Università di Perugia, Perugia, Italy.

^pAlso at LIP6, Sorbonne Université, Paris, France.

^qAlso at Universidade de Brasília, Brasília, Brazil.

^rAlso at Hangzhou Institute for Advanced Study, UCAS, Hangzhou, China.

^sAlso at Università di Pisa, Pisa, Italy.

^tAlso at Central South U., Changsha, China.

^uAlso at Università di Padova, Padova, Italy.

^vAlso at Excellence Cluster ORIGINS, Munich, Germany.

^wAlso at Department of Physics/Division of Particle Physics, Lund, Sweden.

^xAlso at Università della Basilicata, Potenza, Italy.

^yAlso at Università di Siena, Siena, Italy.

^zAlso at Universidad de Alcalá, Alcalá de Henares, Spain.

^{aa}Also at Università di Urbino, Urbino, Italy.